J Fluoresc (2014) 24:1457–1472
DOI 10.1007/s10895-014-1429-5

ORIGINAL PAPER

Synthesis of Novel Carbazole based Styryl: Rational Approach for Photophysical Properties and TD-DFT

Nagaiyan Sekar · Prashant G. Umape · Shantaram Kothavale · Mininath Deshmukh

Received: 7 May 2014 / Accepted: 7 July 2014 / Published online: 13 August 2014
© Springer Science+Business Media New York 2014

Abstract The synthesis and solvatochromic behavior of four novel carbazole based fluorescent styryl dyes were explained. In chlorinated solvents such as DCM and chloroform, these dyes show bathochromic shift in their absorption as well as emission. The styryl dyes **6b** and **6c** show solid state yellow fluorescence. DFT and TD-DFT computations were performed to study structural, molecular, electronic and photophysical properties of these dyes. The computed absorption and emission wavelength values are found to be in good agreement with the experimental results. The photophysical properties of these 1-styryl carbazole dyes are also compared with the recently reported 3-styrl carbazole dyes. The unique behavior of dye 6d is well explained by its optimized geometry found in the excited state. Ratio of ground to excited state dipole moment of the synthesized novel styryl compounds were calculated by Bakhshiev and Bilot-Kawski correlations.

Keywords Carbazole styryl compounds · Solid-state fluorescence · Solvatochromism · Solvatofluorism · TD-DFT

Introduction

Carbazole is found to be electronically very similar to that of diphenylamine. It has a planar structure and can be imagined as the bonded diphenylamine. They are well known as conjugated, good hole transporting, electron-donor and planar compounds [1, 2]. Pyrenyl-functionalized fluorene and carbazole derivatives are used as blue-light emitters [3]. The high-triplet-energy tri-carbazole derivatives are used as host materials for efficient solution-processed blue phosphorescent devices [4]. Carbazole based polymers are important because of their electrical and photoelectrical properties, Such polynorbornenes with pendant carbazole derivatives have been reported as host materials for highly efficient blue phosphorescent organic light-emitting diodes [5, 6]. Since the first commercial organic photoconductor was known to be based on the charge transfer complex between poly (N-vinylcarbazole) (PVK) and 2,4,7-trinitrofluorenone (TNF) there are number of reports concerning the synthesis and photoconductivity of the carbazole-containing polymers [7–10]. They impart thermal and orientation stability to the corresponding polymeric materials [11].

Carbazole can be converted into a nonlinear optical (NLO) chromophores by the introduction of electron withdrawing groups into the 3- and/or 6-position of the carbazole ring [12] It also exhibit ambipolar conductive behavior for electroluminescent devices [13]. Three-photon absorption (3PA) properties of symmetric-type carbazole derivatives show great potential for application in the light-activated therapy and optical limiting devices [14]. The carbazole derivatives having high-glass transition temperatures are used as aggregation-induced emission enhancement materials [15]. The conjugated copolymers of the electron-donating 2, 7-carbazolylene and electron-accepting π-systems were found to be very suitable as a *p*-type semiconductor for bulk heterojunction solar cells [15–20]. Multi-carbazole derivatives (2C-4C) with a twisted and zigzag-shape structure are used for highly efficient dye-sensitized solar cells [21, 22].

Carbazole derivatives are also used as potential antitumor agent and fluorescence marker of cancer cells [23]. Carbazole

Electronic supplementary material The online version of this article (doi:10.1007/s10895-014-1429-5) contains supplementary material, which is available to authorized users.

N. Sekar (✉) · P. G. Umape · S. Kothavale · M. Deshmukh
Tinctorial Chemistry Group, Department of Dyestuff Technology, Institute of Chemical Technology, (Formerly UDCT), Nathalal Parekh Marg, Matunga, Mumbai 400 019, India
e-mail: n.sekar@ictmumbai.edu.in

N. Sekar
e-mail: nethi.sekar@gmail.com

based styryl chromophores show red shifted emission with enhanced fluorescent intensity and are reported as excellent fluorescent probes for biological labeling [24]. They also show unusual large Stokes shift, and excellent thermal stability [25]. The carbazole based styryl derivatives are reported to have luminescent properties, strong two photon absorption and prolonged fluorescence lifetime [25]. The carbazole based styryl derivatives have therefore drawn attention of researchers for their applications in electroluminescent devices [26], dye-sensitized solar cells [27], two photon absorbing materials [28], bioimaging in living cell [29], and non-linear optical devices [30].

In continuation of our ongoing research work in the area of carbazole containing push-pull chromophores [31, 32] we report here push-pull ethylene chromophores derived from 4-methoxy-9-methyl-9*H*-carbazole-1-carbaldehyde (Compound **3**). The photophysical properties and molecular properties of the novel push-pull chromophores have been studied experimentally and supported by DFT and TD-DFT computations.

Experimental Sections

Materials and Equipments

All the commercial reagents and solvents were procured from s. d. fine chemicals (India). The reaction was monitored by TLC using 0.25 mm E-Merck silica gel 60 F_{254} precoated plates, which were visualized with UV light. Melting points were measured on standard melting point apparatus from Sunder industrial product Mumbai, and are uncorrected. The FT-IR spectra were recorded on a JASCO 4100 FT-IR Spectrometer. ^{1}H NMR spectra were recorded on VXR 300 MHz instrument using TMS as internal standard. The visible absorption spectra of the compounds were recorded on a Spectronic Genesys 2 UV-Visible spectrophotometer.

Synthetic Strategy

Synthesis of novel styryl derivatives was carried out by Knoevenagel condensation reaction between compound **3** and different active methylene compounds **(5a-5d)**. The active methylene compounds used are malononitrile **(5a)**, 2-cyanomethyl-1, 3-benzthiazole **(5b)**, 2-(cyanomethyl) benzimidazole **(5c)** and para—nitro benzyl cyanide **(5d)**.

The key intermediate compound **3** was synthesized by methylation of 4-hydoxy carbazole (compound **1**) using two equivalent of methyl iodide to get 4-methoxy-9-methyl-9*H*-carbazole (compound **2**), followed by Vilsmeier formylation of compound **2** giving a mixture of compound **3** and compound **4** (4-methoxy-9-methyl-9*H*-carbazole-3-carbaldehyde). The mixture of compounds **3** and **4** was separated by column chromatography. The pure compound **3** thus obtained was further utilized for synthesis of novel styryl dyes **6a–6d**. Synthetic route of these dyes is well described in Scheme 1 and structures of dyes **6a–6d** are given in Fig. 1.

The synthesized dyes were characterized by FT-IR, ^{1}H-NMR, and mass spectral analysis. FT-IR spectra of dye **6b** show a sharp signal at 2,206 cm^{-1} attributed to the CN stretching. A signal at 1,600 cm^{-1} corresponds to olefinic bond in conjugation with aromatic ring, signal at 1,556 cm^{-1} corresponds to the aromatic C=C stretching. ^{1}H-NMR spectra of the dye **6b** shows a singlet at δ 9.11 corresponding to olefinic proton, six doublets are observed at δ 8.36, 8.27, 8.08, 7.92, 7.44 and 6.86 ppm corresponds to six aromatic protons, two multiplate at δ 7.56–7.48 and 7.34–7.29 attributed to four aromatic protons. Two singlet observed at 4.17 and 4.16 corresponds to six aliphatic protons of N-CH_3 and –OCH_3. Mass spectral analysis of dye **6b** shows M+1 peak at 396, which is in agreement with the molecular weight.

Further, evaluation of photophysical properties of these chromophores **6a–6d** were carried out and ratio of their dipole moments at ground state to the excited state were calculated.

Synthesis and Characterization

Synthesis of Compound **2**

Sodium hydride (5.45 g, 60 %, 136.45 mmol) was charged in 30 ml of dry THF and cooled to 0 °C under nitrogen atmosphere. 9*H*-*C*arbazole-4-ol **1** was dissolved in 30 ml THF and slowly added to the reaction mixture at 0 °C, stirred for 30 min at the same temperature and then methyl iodide (8.70 ml, 136.45 mmol) was added drop-wise into the reaction mixture. The reaction mass thus obtained brought to room temperature and stirred for 2 h under nitrogen atmosphere. Completion of the reaction was monitored by TLC. Excess of sodium hydride is quenched by adding *t*-butyl alcohol under cooling conditions. Solvent was distilled out and cold water was added to the residual mass, which was stirred well and the solid separated was filtered. Crude product thus obtained was purified by column chromatography on silica 60–120 mesh using toluene as eluent to get g of pure product. *Yield = 93 %;* (Melting point = 146–148 °C).

Synthesis of Compound **3**

$POCl_3$ (4.9 ml, 52.00 mmol) was added drop-wise to DMF (17 ml, 219.53 mmol) at 0–5 °C, and stirred for 30 min maintaining the temperature 0–5 °C. Compound **2** (10 g, 47.00 mmol) was dissolved in 20 ml DMF and added drop-wise to the reaction mass within 30 min maintaining temperature between 0 and 5 °C. Stirring was continued for next 20–

Scheme 1 Synthesis of styryl dyes from 4-methoxy-9-methyl-9H-carbazole-1-carbaldehyde

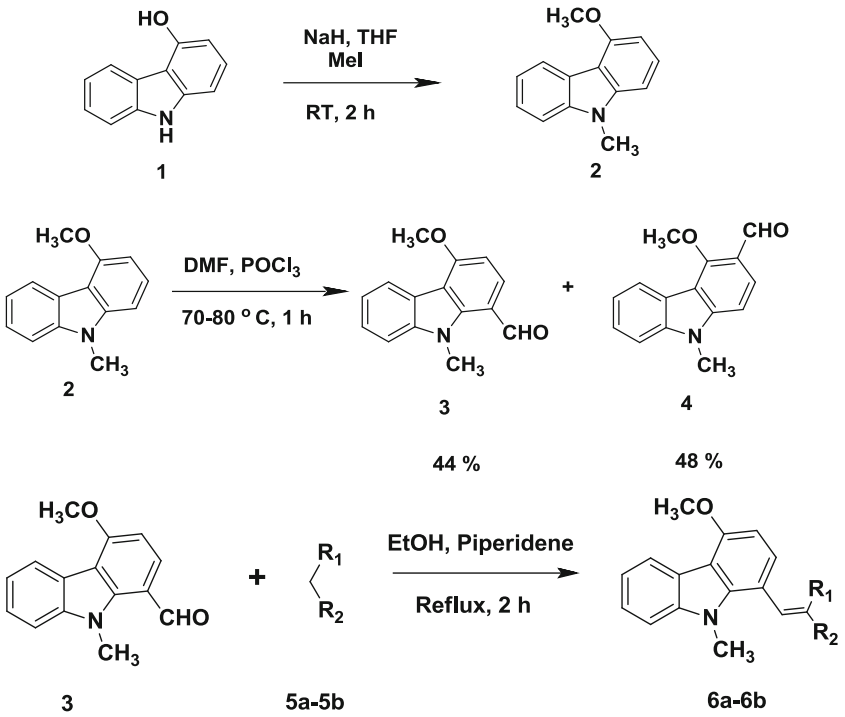

30 min; reaction mixture was then brought to room temperature and heated at 70–75 °C for 1 h. Completion of the reation was monitored by TLC, show formation of two major products. The obtained reaction mass poured into crushed ice stirred well and neutralized with sodium bicarbonate. Precipitate obtained was filtered off and dried well. The crude product contains a mixture of compound **3** and **4.** Separation of these two individual compounds was carried out by column chromatography on silica 100–200 mesh and using toluene as eluent to get compound **3** *Yield= 44 %;* Melting point=134–136 ° C and compound **4** Yield=48 %; Melting point=120–122 °C.

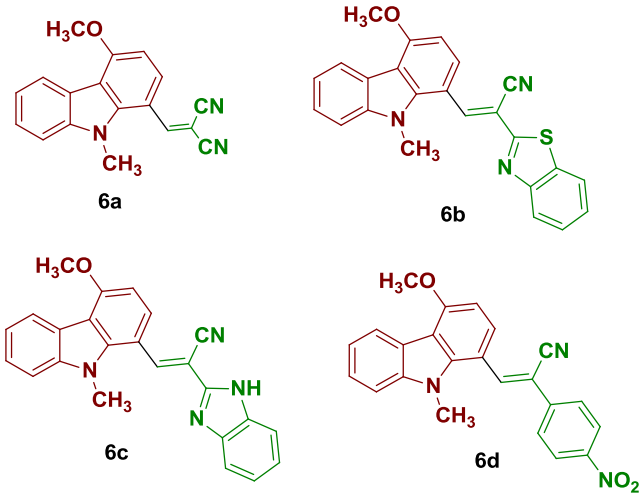

Fig. 1 Structures of the dyes **6a, 6b, 6c** and **6d**

Compound **3** FT-IR showing peak at 1,675 cm^{-1}(C=O), 1,592 cm^{-1}(C=C, aromatic).

^{1}H NMR ($CDCl_3$, 300 MHz)=δ 10.18 (s, 1H), 8.35 (d, 1H, *J*=7.7 Hz), 7.91 (d, 1H, *J*=8.4 Hz), 7.53–7.48 (m, 2H),7.31 (t, 1H, *J*=8.0 Hz), 7.25 (d, 1H, *J*=8.0 Hz), 6.82 (d, 1H, *J*= 8.8 Hz), 4.21 (s, 3H), 4.17 (s, 3H).

Synthesis of 2-((4-methoxy-9-methyl-9H-carbazol-1-yl) Methylene) Malononitrile (Dye **6a)**

Compound **3** (0.57 g, 2.38 mmol) was dissolved in 10 ml ethanol, in which malononitrile (0.17 g, 2.50 mmol) was added at room temperature and stirred. To this reaction mixture catalytic amount of piperidine was added and refluxed for 2 h. Bright yellow colored crystals separated out. Completion of the reaction was monitored by TLC. The resultant reaction mass was filtered off and dried. The crude product was purified by column chromatography using 100–200 mesh silica and toluene as eluent.

Yield=87 %; Melting point=210–212 °C
FT-IR (cm^{-1}): 2,221 cm^{-1} (CN), 1,563 cm^{-1}(C=C, aromatic).
Mass=*m/z* 288 (M+1).

^{1}H NMR ($CDCl_3$, 500 MHz)=δ 8.45 (s, 1H), 8.32 (d, 1H, *J*=7.5 Hz), 8.27 (d, 1H, *J*=8.5 Hz), 7.53 (t, 1H, *J*=7, 7.5 Hz), 7.42 (d, 1H, *J*=8 Hz),7.34 (t, 1H, *J*=8, 7 Hz), 6.84 (d, 1H, *J*= 9 Hz), 4.18 (s, 3H), 4.03 (s, 3H).

Synthesis of (E)-2-(benzo[d]thiazol-2-yl)-3-(4-methoxy-9-methyl-9H-carbazol-1-yl) Acrylonitrile (Dye **6b***)*

Compound **3** (0.5 g, 2.09 mmol) was dissolved in 10 ml ethanol. 2-Cyanomethyl-1, 3-benzothiazole (0.36 g, 2.09 mmol) was added to it and stirred. To this mixture catalytic amount of piperidine was added and refluxed for 2 h. Yellow colored product separate out as reaction proceed, completion was monitored by TLC. The solid separated was filtered off and dried well, obtained crude product was purified by column chromatography using silica of mesh size 100–200, gradient mixture of EtOAc and toluene was used as eluent system.

Yield=79 %; Melting point=201–204 °C
FT-IR (cm^{-1})=2,206 cm^{-1} (CN), 1,600 cm^{-1} (C=C, olefinic) 1,556 cm^{-1} (C=C, aromatic)
Mass=*m/z* 396 (M+1).

^{1}H NMR ($CDCl_3$, 300 MHz)=δ 9.11 (s, 1H), 8.36 (d, 1H, *J*=7.8 Hz), 8.27 (d, 1H, *J*=8.1 Hz), 8.08 (d, 1H, *J*=7.7 Hz), 7.92 (d, 1H, *J*=8.1 Hz), 7.56–7.48 (m, 2H), 7.34–7.29 (m, 2H), 6.86 (d, 1H, *J*=6.86 Hz), 4.17 (s, 3H), 4.17 (s, 3H).

Synthesis of (E)-2-(1H-benzo[d]imidazol-2-yl)-3-(4-methoxy-9-methyl-9H-carbazol-1-yl) Acrylonitrile (Dye **6c)**

Compound **3** (0.5 g, 2.09 mmol) and 2-(cyanomethyl) benzimidazole (0.33 g, 2.09 mmol) were dissolved in 10 ml ethanol. To this mixture catalytic amount of piperidine was added and refluxed for 2 h. Yellow colored product separated out as reaction proceeds. Completion of reaction was monitored by TLC. Reaction mass thus obtained was filtered and crude product was dried. Purification of dye **6c** was carried out by column chromatography using silica of mesh size 100–200, gradient mixture of EtOAc and toluene was used as eluent system.

Yield=61 %; Melting point=248–249 °C
FT-IR (cm^{-1})=2,207 cm^{-1} (CN), 1,578 cm^{-1} (C=C, aromatic).
Mass=*m/z* 379 (M+1).

^{1}H NMR ($CDCl_3$, 300 MHz)=δ 8.67 (s, 1H), 8.35 (d, 1H), 8.23 (d, 1H, *J*=8.7 Hz), 7.79–7.87 (m, 3H) 7.52 (d, 1H, *J*= 9.3 Hz),7.27 (m, 3H), 6.85 (d, 1H, *J*=8.7 Hz), 5.31(s, 1H), 4.19 (s, 3H), 4.18 (s, 3H).

Synthesis of (Z)-3-(4-methoxy-9-methyl-9H-carbazol-1-yl)-2-(4-nitrophenyl) Acrylonitrile (Dye **6d)**

Compound **3** (0.5 g, 2.09 mmol) and para-nitro benzyl cyanide (0.36 g, 2.09 mmol) were dissolved in 10 ml ethanol. To this mixture catalytic amount of piperidine was added and refluxed for 2 h. Red colored crystals separated out as reaction proceed; completion of reaction was monitored by TLC. The crude product **6d** was

Table 1 Experimental and computed absorption and emission of the dye **6a** with their respective quantum yields in different solvents

Solvents	Experimental			Computed (TD-DFT)						Φ
	λ_{max}[a] nm (ε)	λ_{max}[b] nm (Intensity)	Stokes shift	Vertical[c] excitation (nm)	*f*[d]	% Orbital contribution	%D[e]	TD-DFT emission (nm)	%D[f]	
THF	431(24,450)	502	71	435.02	0.3971	96	0.25	468.36	6.69	0.0007
EtOAc	431(23,243)	498	68	433.74	0.3894	96	0.51	466.87	6.25	0.0105
DCM	437(24,737)	501	64	435.83	0.4013	97	1.45	469.45	6.29	0.0008
Chloroform	440(23,215)	501	61	434.6	0.4071	97	2.46	464.88	7.20	0.0021
Acetone	431(26,921)	511	80	435.5	0.3849	96	0.08	472.68	7.49	0.0028
MeOH	431(23,875)	517	78	435.12	0.3770	96	0.14	473.14	8.38	0.0080
Ethanol	434(24,737)	507	73	435.72	0.3854	96	0.73	473.66	6.67	0.0021
Acetonitrile	428(22,439)	517	89	435.54	0.3810	96	0.63	473.81	8.35	0.0120
DMF	434(19,307)	514	80	448.39	0.6082	94	3.31	473.88	7.80	0.0087

Φ Quantum yield at various solvents, *THF* Tetrahydrofuran, *EtOAc* Ethyl acetate, *DCM* Dichloromethane, *MeOH* Methanol, *DMF* N, N-Dimethylformamide

[a] Experimental absorption wavelength

[b] Experimental emission wavelength

[c] Computed absorption wavelength

[d] Oscillator strength

[e] % Deviation between experimental absorption and vertical excitation computed by DFT

[f] % Deviation between experimental emission and computed (TD-DFT) emission

Table 2 Experimental and computed absorption and emission of the dye **6b** with their respective quantum yields in different solvents

Solvents	Experimental			Computed (TD-DFT)						Φ
	λ_{max}[a] nm (ε)	λ_{max}[b] nm (intensity)	Stokes shift	Vertical[c] excitation (nm)	f[d]	% Orbital contribution	%D[e]	TD-DFT emission (nm)	%D[f]	
THF	431(14,355)	503	72	453.02	0.824	96	5.10	495.53	1.48	0.0016
EtOAc	431(11,231)	492	61	451.67	0.817	96	4.79	492.71	0.14	0.0768
DCM	434(14,632)	503	69	453.87	0.828	96	4.57	497.59	1.07	0.0012
Chloroform	434(12,220)	513	79	452.64	0.840	96	4.29	489.01	4.67	0.0019
Acetone	425(13,169)	509	84	453.44	0.806	96	6.69	503.77	1.02	0.0026
MeOH	428(13,209)	510	82	452.99	0.795	96	5.83	504.66	0.84	0.0020
Ethanol	428(13,802)	511	83	453.65	0.806	96	5.99	505.67	1.23	0.0063
Acetonitrile	425(12,101)	507	82	453.45	0.800	96	6.69	505.95	0.20	0.0015
DMF	431(17,045)	532	101	455.58	0.825	97	5.70	506.08	4.87	0.0048

Φ Quantum yield at various solvents, *THF* Tetrahydrofuran, *EtOAc* Ethyl acetate, *DCM* Dichloromethane, *MeOH* Methanol, *DMF* N, N-Dimethylformamide

[a] Experimental absorption wavelength

[b] Experimental emission wavelength

[c] Computed absorption wavelength

[d] Oscillator strength

[e] % Deviation between experimental absorption and vertical excitation computed by DFT

[f] % Deviation between experimental emission and computed (TD-DFT) emission

isolated by filtration and dried. Purification of dye **6d** was carried out by column chromatography using silica of mesh size 100–200, gradient mixture of EtOAc and toluene was used as eluent system.

Yield=61 %; Melting point=140–142 °C
FT-IR (cm^{-1})=2,207 cm^{-1} (CN), 1,593 cm^{-1} (C=C, aromatic), 1,555 cm^{-1} (NO_2, aromatic)
Mass=*m/z* 384 (M+1).

Table 3 Experimental and computed absorption and emission of the dye **6c** with their respective quantum yields in different solvents

Solvents	Experimental			Computed (TD-DFT)						Φ
	λ_{max}[a] nm (ε)	λ_{max}[b] nm (Intensity)	Stokes shift	Vertical[c] excitation (nm)	f[d]	% Orbital contribution	%D[e]	TD-DFT emission (nm)	%D[f]	
THF	401(17,294)	455	54	435.02	0.849	96	8.48	483.79	6.32	0.0006
EtOAc	401(16,310)	473	72	433.74	0.841	96	8.16	481.06	1.70	0.0276
DCM	407(32,506)	504	97	435.83	0.852	97	7.08	485.79	3.61	0.0010
Chloroform	410(15,818)	476	66	434.6	0.863	97	6.00	477.40	0.29	0.0008
Acetone	404(19,716)	487	83	435.5	0.829	96	7.79	491.64	0.95	0.0003
MeOH	410(16,575)	482	72	435.12	0.818	96	6.12	492.46	2.17	0.0022
Ethanol	410(17,369)	482	72	435.72	0.829	96	6.27	493.40	2.42	0.0005
Acetonitrile	404(17,218)	468	64	435.54	0.822	96	7.80	493.66	5.42	0.0010
DMF	407(16,726)	534	127	437.52	0.846	97	7.49	493.77	7.53	0.0239

[a] Experimental absorption wavelength

[b] Experimental emission wavelength

[c] Computed absorption wavelength

[d] Oscillator strength

[e] % Deviation between experimental absorption and vertical excitation computed by DFT

[f] % Deviation between experimental emission and computed (TD-DFT) emission

Φ Quantum yield at various solvents, *THF* Tetrahydrofuran, *EtOAc* Ethyl acetate, *DCM* Dichloromethane, *MeOH* Methanol, *DMF* N, N-Dimethylformamide

Table 4 Experimental and computed absorption and emission of the dye **6d** with their respective quantum yields in different solvents

Solvents	Experimental			Computed (TD-DFT)						Φ
	λ_{max}[a] nm (ε)	λ_{max}[b] nm (intensity)	Stokes shift	Vertical[c] excitation (nm)	f[d]	% Orbital contribution	%D[e]	TD-DFT emission (nm)	%D[f]	
THF	431(17,395)	528	97	509.76	0.559	99	18.27	[g]	–	0.0176
EtOAc	425(24,422)	546	121	507.52	0.554	99	19.41	[g]	–	0.0020
DCM	434(28,799)	540	106	511.24	0.562	99	17.79	586.07	8.53	0.0075
Chloroform	440(26,495)	541	101	506.98	0.573	99	15.22	586.88	8.48	0.0599
Acetone	425(23,769)	541	116	512.81	0.543	99	20.66	585.07	8.14	0.0017
MeOH	428(19,660)	512	84	512.95	0.534	99	19.84	[g]	–	0.0039
Ethanol	428(22,847)	534	106	513.25	0.542	99	19.91	584.90	9.53	0.0017
Acetonitrile	425(22,924)	520	95	513.44	0.538	99	20.80	584.63	12.43	0.0015
DMF	428(22,195)	541	113	533.84	0.722	98	24.72	584.61	8.06	0.0022

Φ Quantum yield at various solvents, *THF* Tetrahydrofuran, *EtOAc* Ethyl acetate, *DCM* Dichloromethane, *MeOH* Methanol, *DMF* N, N-Dimethylformamide

[a] Experimental absorption wavelength

[b] Experimental emission wavelength

[c] Computed absorption wavelength

[d] Oscillator strength

[e] % Deviation between experimental absorption and vertical excitation computed by DFT

[f] % Deviation between experimental emission and computed (TD-DFT) emission

[g] The excited state optimization take unusually longer time and hence not done

^{1}H NMR ($CDCl_3$, 300 MHz)=δ 8.39 (s, 1H), 8.33–8.36 (m, 3H), 8.06 (d, 1H, *J*=8.7 Hz), 7.93 (d, 1H, *J*=7.2 Hz), 7.89–7.87 (m, 2H), 7.41–7.37 (m, 2H), 6.84 (d, 1H, *J*= 8.7 Hz), 4.18 (s, 3H), 4.06 (s, 3H).

Computational Methods

Density functional theory computations [B3LYP/6-31G (d)] were carried out to study the geometrical and electronic properties of the synthesized molecules. The ground state geometry of all the styryl derivatives in their C1 symmetry was optimized using DFT [33] in the gas phase. The B3LYP functional with 6-31G (d) basis set was used for performing the calculations. The optimized structures corresponds to local minima on the energy surface was verified by performing vibrational analysis using the same B3LYP/6-31G (d) method. The vertical excitation energies and oscillator strengths were obtained by using TD-DFT at the same hybrid functional and basis set [34] for obtaining the lowest 10 singlet-singlet transitions at the optimized ground state equilibrium geometries. The difference between the energies of the optimized geometries at first singlet excited state and ground state was used to calculate the emission [35–37].

All the computations in solvents of different polarities were carried out using the Self-Consistent Reaction Field (SCRF) under the Polarizable Continuum Model (PCM) [38]. Similarly vertical electronic excitation spectra, including wavelengths, oscillators strengths, and main configuration assignment were also investigated using the same TDDFT-PCM model. Frequency computations were also carried out on Franke-Condon excited state of the dyes. [39, 40].

Results and Discussion

Photo-Physical Properties of Styryl Dyes 6a–6d

The synthesized dyes **6a–6d** are of the push-pull chromophoric systems, with *N* and O-methyl unit acts as donor and active

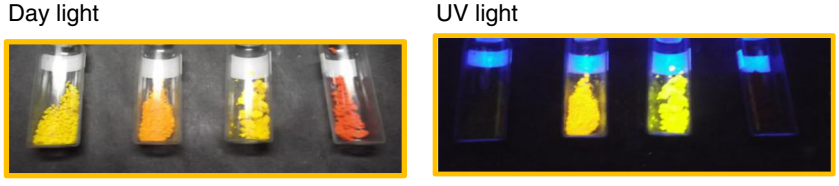

Compound 6a, 6b, 6c and 6d (left to right)

Fig. 2 Photographs of dyes **6a-6d** in day light and UV-light to show solid state fluorescence

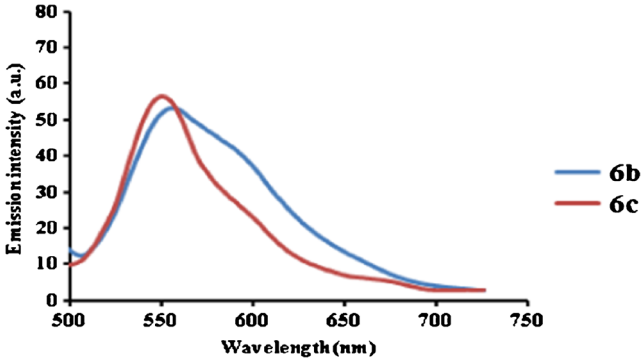

Fig. 3 Overlay Solid state fluorescence spectrum of dyes **6b** and **6c**

methylene unit as acceptor. From literature, it is evident that such moieties possess excellent photo physics. Here, we have investigated the photo physical properties of these dyes.

The absorption maxima of dyes **6a–6d** ranges from 401 to 440 nm and emission maxima ranges from 468 to 546 nm; with Stokes shift ranging between 61 to 127 nm. Figure 4 represents overlay absorption spectra of dyes **6a–6d** in DCM solvent. After replacement of benzimidazole unit with benzothiazole and para-nitro benzyl unit with cyano group bathochromic shift in absorption maxima while hypsochromic shift in emission maxima was observed (Fig. 6). The comparative experimental as well as computational absorption and emission data of these dyes in different solvents of different polarities are tabulated in Tables 1, 2, 3, and 4 with their relative quantum yields in different solvents.

The dyes **6b** and **6c** show very good yellow solid state fluorescence (Fig. 2). The overlay solid state fluorescence spectrum of dyes **6b** and **6c** was also taken **(**Fig. 3 and Table 5**).**

Solvatochromism and Solvatofluorism

Microenvironment such as solvent polarity and viscosity greatly affects the absorption, emission and quantum yield of the fluorescent compounds. Here, the UV-Vis absorption, fluorescence emission and fluorescence excitation spectra of the synthesized dyes **6a–6d** are recorded at concentration 1×10^{-6} mol L^{-1} in different solvents of varying polarity in order to check the effect of solvent parameters such as solvent polarity. The collected data is summarized in Tables 1, 2, 3 and 4 and the obtained spectra are shown in Figs. 4, 5, 6 and 7.

The solvatochromism data shows that all four dyes are showing bathochromic shift in their absorption in chlorinated

Table 5 Solid state fluorescence data of dye **6b** and **6c**

Dye	Abs. λmax (nm)	Emis. (nm)	Emis. intensity
6b	431	565	53.13
6c	401	550	56.59

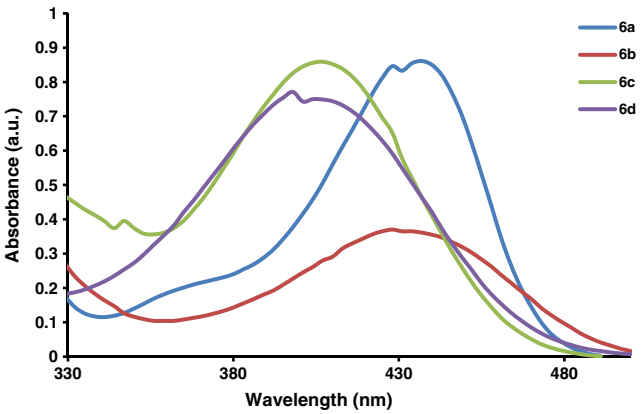

Fig. 4 Absorption spectra of dyes **6a-6d** in dichloromethane

solvents such as Chloroform and DCM. The dye **6a** absorbs around 428 to 434 nm in majority of solvents, but in chlorinated solvents such as DCM and chloroform it shows bathochromic shift and absorbs at 437 nm and 440 nm respectively (Table 1). Dy**e 6a** is showing highest absorption intensity in MeOH and lowest one in DMF (Fig. 5). Similarly, dye **6b** absorbs from 425 to 434 nm in all mentioned solvents and is also showing slight bathochromic shift in chlorinated solvents (Table 2). Here, dye **6b** shows highest absorption intensity in DCM and THF, while in EtOAc it absorbs with lowest absorbance (Figure S1).

The solvatochromism study of dye **6c** (Table 3**)** shows that there is no specific trend with change in solvent polarity. The overlay absorption spectra for dye **6c** as shown in Figure S2 is clearly indicating unique and strong absorbance in DCM as compared to all other remaining solvents. Dye **6d** also shows red shifted absorption maxima in chloroform at 440 nm, while in all other remaining solvents it absorbs between 425 to 434 nm (Table 4). The overlay spectra for dye **6d** as shown in Figure S3 is also indicating strong absorption in chloroform and DCM solvents and lowest one in THF solvent.

The dyes **6a–6d** are also evaluated for their fluorescence emission properties and the obtained data is summarized in Tables 1, 2, 3, and 4. The overlay emission spectra of all the

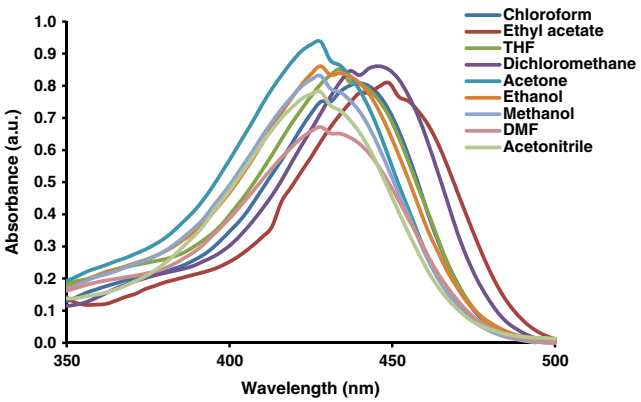

Fig. 5 Absorption spectra of dye **6a** in different solvents

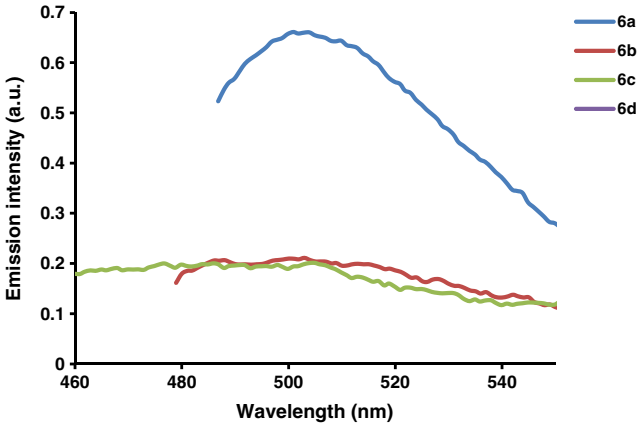

Fig. 6 Emission spectra of dyes **6a-6d** in dichloromethane

synthesized dyes **6a–6d** in DCM shown in Fig. 6 where a noticeable strong emission for dye **6a** is observed which is due to the strong electron withdrawing di-cyano substituent's at the terminal end. In case of other dyes which emits with emission intensity below 0.2 a.u; distortion in planarity may be one of the reason behind these characteristics. Dye **6a** emits from 498 to 517 nm in different solvents (Table 1**)**, it is envisaged that the emission maxima shows red shifted emission in polar solvents such as MeOH (517 nm), DMF (514 nm) and blue shifted emission in non polar solvents such as THF (502 nm) and EtOAc (498 nm). Overlay emission spectra of dye **6a** in different solvents (Fig. 7**)** shows strong emission characteristics in DMF, acetone, acetonitrile, MeOH and EtOAc, while in other solvents emission intensity below 0.5 a.u. is observed. In case of dye **6b** a remarkable bathochromic shift at 532 nm is seen in DMF, while in other solvents emission is observed between 492 nm in EtOAc to 513 nm in chloroform (Table 2). Here, also strongest emission intensity is observed in DMF, while in acetone, ethanol, acetonitrile and MeOH acceptable emission intensities are observed (Figure S4).

The emission range of dye **6c** in different solvents is found to be 455 to 534 nm. In DCM and DMF noticeable bathochromic shifts are observed at 534 and 504 nm respectively. While in acetonitrile and THF remarkable hypsochromic shifts are observed at 468 and 455 nm respectively (Table 3). Strongest

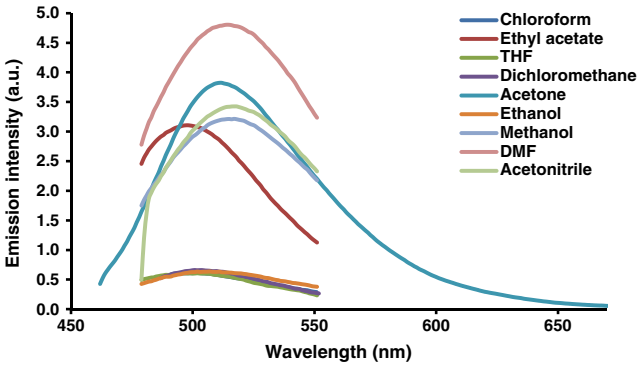

Fig. 7 Emission spectra of dye **6a** in different solvents

emission for dye **6c** is observed in DMF and weakest one in DCM **(**Figure S5**).** Dye **6d** has the highest emission in the series of dyes **6a–6d** ranges from 512 to 546 nm. This dye has highest emission in EtOAc at 546 nm and lowest one in MeOH at 512 nm (Table 4). Here, strongest emission is observed in THF, while weakest one in acetonitrile is observed **(**Figure S6**).**

Stokes Shifts of the Dyes

The calculated Stokes shifts of these dyes from Tables 1, 2, 3, and 4 indicate that largest Stokes shift of 127 nm is observed for dye **6c** in DMF while in other solvents Stokes shift of dye **6c** falls in between 54 to 97 nm (Table 3). Here, dye **6d** has largest Stokes shifts in majority of solvents than other synthesized chromophores and it ranges from 84 nm in MeOH to 121 nm in EtOAc. In case of dyes **6a** and **6b**, the Stokes shifts increases with solvent polarity. For dye **6a** it increases from 61 nm in chloroform to 89 nm in acetonitrile (Table 1). Similarly, dye **6b** shows increase in Stokes shift from 61 nm in EtOAc to 101 nm in DMF (Table 2).

Quantum Yields of the Dyes

As quantum yield of fluorescent compounds is getting affected due to the solvent polarity, a relative quantum yield of the synthesized dyes **6a–6d** were calculated in solvents of different polarities so as to analyze the effect of different solvents on the quantum yield **(**Tables 1, 2, 3, and 4**)**. Fluorescein was used as a reference standard.

Dye **6a** shows good quantum yield of 0.0120 and 0.0105 in acetonitrile and EtOAc, while lowest quantum yield of 0.0007 and 0.0008 in THF and DCM respectively (Table 1). Dye **6b** shows excellent quantum efficiency in EtOAc of 0.0768 which is the highest quantum yield among all synthesized derivatives **6a–6d** in all mentioned solvents. Here, lowest value of quantum yield 0.0012 is observed in DCM (Table 2). Dye **6c** is showing highest quantum yield of 0.0276 in EtOAc and lowest value of 0.0003 is obtained in acetone and is the lowest value of quantum yield of these synthesized dyes. Dye **6c** also shows good quantum efficiency 0.0239 in DMF. For dye **6d**, the relative quantum yield obtained in different solvents enlighten that it fluoresces with quantum efficiency 0.0599 in chloroform and 0.176 in THF while in acetonitrile it has lowest value of 0.0015.

Comparative Photo-Physical Properties of the 4-methoxy N-methyl Carbazole 1-styryl and 4-methoxy N-methyl Carbazole 3-styryl Derivatives

The absorption and emission maximum of 4-methoxy N-methyl carbazole 1-styryl and 4-methoxy N-methyl carbazole 3-styryl derivatives [41] were compared and it is observed that for all three dyes in all solvents 1-styryl derivatives are showing red shifted absorption as well as emission than the corresponding

Table 6 Comparative photophysical properties of the 4-methoxy N-methyl carbazole 1-styryl and 4-methoxy N-methyl carbazole 3-styryl (given in bracket) based dyes in different solvents

Solvent	Dye 6b (6a)		Dye 6c (6b)		Dye 6d (6c)	
	λabs, nm	λems, nm	λabs, nm	λems, nm	λabs, nm	λems, nm
THF	431(419)	503(488)	401(395)	455(429)	431(413)	528(548)
EtOAc	431(416)	492(484)	401(395)	473(479)	425(413)	546(547)
DCM	434(419)	503(486)	407(398)	504(459)	434(419)	540(593)
Chloroform	434(422)	513(486)	410(398)	476(467)	440(419)	541(481)
Acetone	425(419)	509(485)	404(395)	487(480)	425(413)	541(540)
MeOH	428(419)	510(485)	410(395)	482(480)	428(413)	512(536)
Ethanol	428(422)	511(490)	410(398)	482(481)	428(416)	534(552)
Acetonitrile	425(416)	507(487)	404(392)	468(480)	425(413)	520(540)
DMF	431(425)	532(505)	407(395)	534(488)	428(419)	541(541)

3-styryl derivatives. (Table 6) The dye **6d** (1-styryl derivative) is however exceptionally showing blue shifted emission than the corresponding dye **6c** (3-styryl derivative) which is due to the change in geometry of the withdrawing para-nitro benzyl moiety which turns completely perpendicular to the donating carbazole ring in the excited state causing improper charge delocalization. This is not observed in the case of dye **6c** (3-styryl derivative) and hence it is showing better charge delocalization than dye **6d** (1-styryl derivative). The overall red shifted absorption as well as emission for 1-styryl derivatives where withdrawing moieties are positioned at para position to the donating methoxy substituent suggesting that methoxy group must be acting as supporting donor to the main N-methyl donating center. Figure 8 shows the structure of two different positional styryl derivatives of 4-methoxy 9-methyl carbazole.

Determination of Dipole Moment by Solvatochromic Method

The synthesized dyes **6a–6d** are push-pull type of chromophores, wherein *N*-methyl carbazole unit acts as a donor terminal and cyano, benzthiazole, benzimidazole and para-nitro benzyl unit acts as an acceptor end. Such type of molecules show change in the dipole moment during transition from ground state S_0 to excited state S_1. Such phenomenon is observed due to intramolecular charge transfer between donor and acceptor unit. Out of several methods available for calculation of ground state and excited state dipole moments, we have calculated ratio of excited state dipole moment to the ground state dipole moment based on solvatochromic method. This method is a linear correlation between absorption and emission wavelengths in cm^{-1}, and solvent polarity functions were obtained by Bakhshiev and Kawski-Chamma-Viallet [42–45] (Figs. 9 and 10).

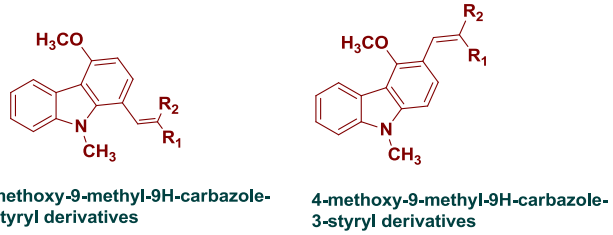

Fig. 8 Structure of two different carbazole based styryl derivatives

Calculations

The solvent polarity functions $f_1(\varepsilon, \eta)$ and $f_2(\varepsilon, \eta)$ for the respective solvent were calculated using Bakhshiev and Bilot-Kawski derivations by substituting values of dielectric constant and refractive index of respective solvents. The values obtained are summarized in Table 7. The absorption and emission maxima obtained are converted to wave number (cm^{-1}). Their Stokes shift and arithmetic mean of absorption and emission maxima $\left(\bar{\nu}_a + \bar{\nu}_f\right)/2$ in cm^{-1} are tabulated in Table 8.

The slope values m_1 obtained by plotting graph of $f_1(\varepsilon, \eta)$ verses Stokes shift in cm^{-1} and slope values m_2 obtained by plotting graph of $f_2(\varepsilon, \eta)$ verses $\left(\bar{\nu}_a + \bar{\nu}_f\right)/2$ in cm^{-1} are summarized in Table 8. From these slope values m_1 and m_2 ratio of excited state dipole moment to the ground state dipole moment was calculated. The final values of ratio of excited state dipole moment to the ground state dipole moment are summarized in Table 9.

The calculated values of ratio of excited state dipole moment to the ground state dipole moment demonstrates that for all these dyes **6a–6d** the ground state is more polarized than the excited state. Such more polarized ground state than the excited state is observed due to efficient charge transfer occurred in the ground state between donor and acceptor terminals, while such efficient charge transfer is hindered in the excited state.

Computational Results

Optimized Geometries of the Dyes

The resulting optimized geometries of the dyes **6a, 6b, 6c** and **6d** were obtained in the ground state having

Table 7 Solvatochromism data and solvent polarity parameters of dyes **6a–6d** with the calculated values of f_1 (ε, η) and f_2 (ε, η)

Solvent	Dye	$\bar{\nu}_a$ (cm_{-1})	$\bar{\nu}_f$ (cm_{-1})	$\Delta\bar{\nu}$ (cm_{-1})	$\frac{(\bar{\nu}_a+\bar{\nu}_f)}{2}$	ε	η	$f_1(\varepsilon,\eta)$	$f_2(\varepsilon,\eta)$
Chloroform	6a	22,727	19,960	2,767	21,344	4.81	1.446	0.371	0.4876
	6b	23,041	19,493	3,548	21,267				
	6c	24,390	21,008	3,382	22,699				
	6d	22,277	18,484	4,243	20,606				
EtOAc	6a	23,202	20,080	3,121	21,641	6.02	1.372	0.4891	0.4979
	6b	23,202	20,325	2,876	21,763				
	6c	24,938	21,142	3,796	23,039				
	6d	23,529	18,315	5,214	20,922				
THF	6a	23,202	19,920	3,281	21,561	7.58	1.407	0.5491	0.5511
	6b	23,202	19,881	3,321	21,541				
	6c	24,938	21,978	2,960	23,458				
	6d	23,202	18,939	4,246	21,071				
DCM	6a	22,883	19,960	2,923	21,422	8.93	1.424	0.5903	0.583
	6b	23,041	19,881	3,161	21,461				
	6c	24,570	19,841	4,729	22,206				
	6d	23,041	18,518	4,523	20,780				
Acetone	6a	23,202	19,569	3,632	21,386	21.01	1.359	0.7925	0.6406
	6b	23,529	19,646	3,883	21,588				
	6c	24,752	20,534	4,219	22,643				
	6d	23,529	18,484	5,045	21,007				
Ethanol	6a	23,041	19,724	3,318	21,383	24.30	1.361	0.8117	0.6516
	6b	23,364	19,569	3,795	21,467				
	6c	24,390	20,747	3,643	22,568				
	6d	23,364	18,727	4,638	21,045				
MeOH	6a	23,202	19,342	3,859	21,272	33.70	1.329	0.8575	0.6529
	6b	23,364	19,607	3,757	21,486				
	6c	24,390	20,747	3,643	22,568				
	6d	23,364	18,484	4,880	20,924				
DMF	6a	23,041	19,455	3,586	21,248	38.25	1.430	0.8395	0.7114
	6b	23,202	18,796	4,405	20,999				
	6c	24,570	18,727	5,843	21,648				
	6d	23,364	19,231	4,299	21,380				
Acetonitrile	6a	23,364	19,342	4,022	21,353	35.94	1.344	0.8593	0.664
	6b	23,529	19,723	3,805	21,627				
	6c	24,752	21,367	3,385	23,060				
	6d	23,529	19,231	4,299	21,380				

planar arrangement of the carbazole moiety with the withdrawing malononitrile in case of **6a** compound while non-planar arrangement of the carbazole moiety with the withdrawing 2-cyanomethyl-1,3-benzthiazole (**6b**), 2-(cyanomethyl)benzimidazole **(6c)** and para-nitro benzyl cyanide (6d) compounds.

The optimized geometry of dye **6a** is such that it has a small twist dihedral angle of 6.10 ^{0} along C12-C29-C31-C32

Table 8 Slope and constant obtained from the graphs in Figs. 9 and 10 for dyes **6a–6d**

Dye	Slope 1 (m_1)	Constant	Correlation coefficient	Slope 2 (m_2)	Constant	Correlation coefficient
6a	1,976	2,038	0.7633	−1,112	22,073	0.4688
6b	1,738	2,427	0.5128	−962	22,048	0.1159
6c	1,451	2,962	0.0953	−3,489	24,764	0.2735
6d	−160	4,658	0.0045	1,910	19,866	0.3182

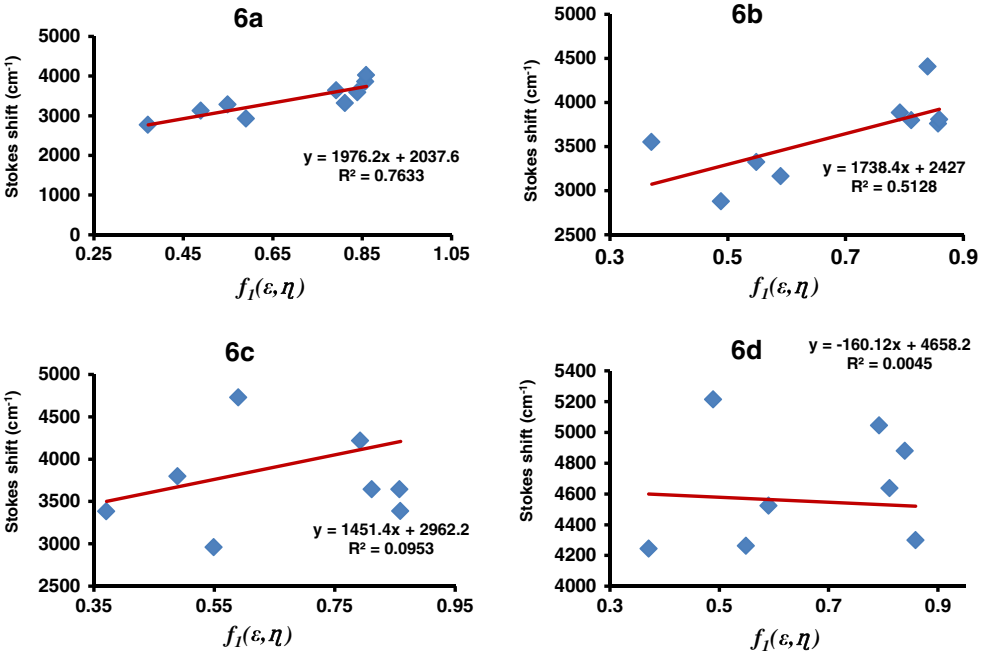

Fig. 9 Plot of Stokes shift $\Delta\bar{\nu}$ with Bakhshiev's polarity parameter f_1 (ε, η) for dyes **6a-6d**

between the carbazole ring and the attached electron withdrawing carbon chain. It is the smallest dihedral angle among all the dyes. The dye **6d** showed highest twist angle among the four dyes of angle 9.55°. The dyes **6b** and **6d** showed dihedral angle of 8.06° and 9.36° along the same C12-C29-C31-C32 carbon chain **(**Table S7**).** In all four dyes decrease in bond angle of C12-C29-C31 was observed when we go from ground to excited state geometry which was maximum 5.4 ^{0} in the case of dye **6d (**Table S6**).**

The ground state optimized geometries of dyes **6a–6d** are not changed much when we go from gas to solvent phase. In case of **dye 6b**, sulphur atom of the thiazole withdrawing moiety is pointed towards the carbazole ring and the thiazole ring becomes more planar with the carbazole unit in its excited state as compared to its ground state geometry in chloroform solvent. In case of dye **6d** the para-nitro benzyl cyanide withdrawing moiety is turned completely perpendicular to the carbazole unit in its excited state as compared to its ground state geometry in all solvents.

All four dyes show variation in their bond length when we go from ground to excited state optimized geometry in chloroform solvent which is shown in Table S5**.** Decrease in bond

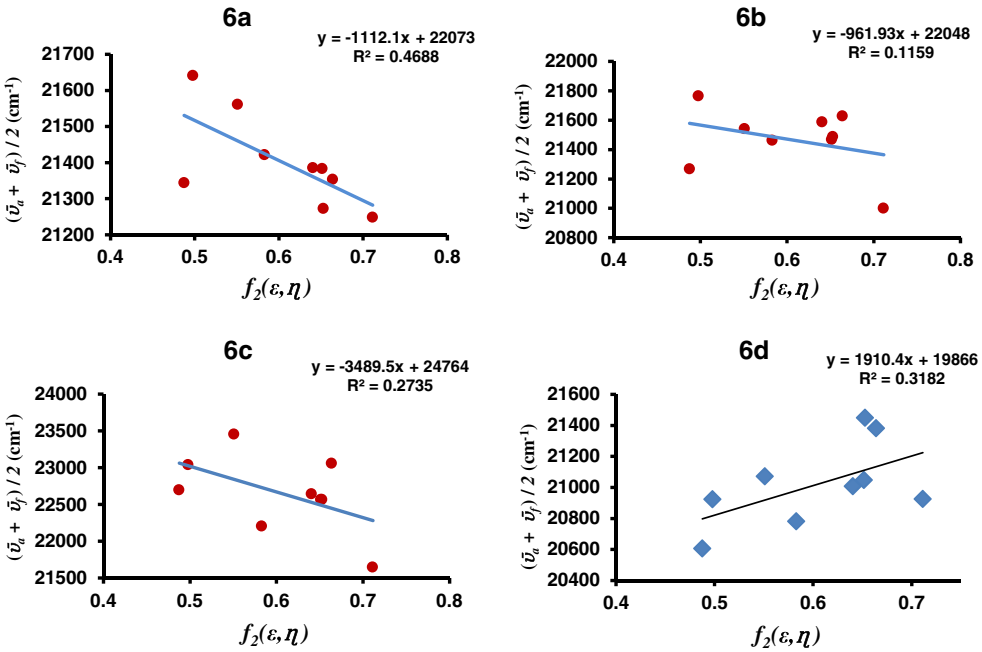

Fig. 10 Plot of Stokes shift $\Delta\bar{\nu}$ with solvent polarity parameter f_2 (ε, η) for dyes **6a-6d**

Table 9 Excited state and ground state Dipole moment (in Debye) ratio value for dyes **6a–6d**

Dye	$\lvert m_1+m_2 \rvert$	$\lvert m_1-m_2 \rvert$	$\frac{\mu_e}{\mu_g}$
6a	864	3,088	0.28
6b	776	2,700	0.29
6c	2,038	4,941	0.41
6d	850	1,170	0.73

length for C4-N19 and increase in bond length for C11-N19 in the case of all four dyes was observed. As expected decrease in bond length for C12-C29 was observed in the case of dye **6b** and **6c** but it was unexpectedly opposite in the case of dye **6a** and **6d** suggesting the improper charge delocalization in these two dyes. Increase in bond length for C29-C31 was observed in all four dyes as per expectation. Again dye **6d** is not showing the shortening of the bond length of C31-C32 and lengthening of bond length of C32-C33, but all four dyes showing shortening of the bond length of C31-C35 Fig. 11.

Mulliken Charge Distribution of Dyes 6a–6d

The Mulliken charge distribution in ground state (Chloroform solvent) on selected atoms of the dyes **6a**, **6b**, **6c** and **6d** are shown in Table 10. In the excited state, the dye **6b** showed decrease in the negative charge on atom N19 and O24; and increase on N33 and N34 which suggest charge delocalization in the molecule from nitrogen atom of carbazole donor to

dicyanovinyl acceptor moiety. Same charge delocalization was observed for dye **6c** also. In the case of dye **6a** and dye **6d** there is no decrease in negative charge on atom N19 and O24, but increase in negative charge on atom N33 and N34, suggesting improper delocalization of charge as compared to dye **6b** and dye **6c**. In all four dyes positive charge on atom C31 was observed to which all electron withdrawing moieties are attached. In dye **6d** the improper charge delocalization is supported by its optimized geometry obtained in the excited state where the withdrawing para-nitro benzyl cyanide moiety found completely perpendicular to the carbazole ring. Fig. S11-S14 and Table 10 represent Mulliken charge distribution on atoms in the molecule.

Electronic Vertical Excitation Spectra (TDDFT)

The computed vertical excitations of dye **6a, 6b** and **6c** were found minimum for EtOAc and maximum for DMF solvent, while in the case of dye **6d** it is minimum (506.98 nm) for chloroform solvent and maximum (533.84 nm) for DMF solvent. Experimental absorption maxima was found highest in chloroform solvent for all four dyes while lowest in EtOAc (431 nm) for dye **6a**, acetone (425 nm) for dye **6b**, THF (401 nm) for dye **6c** and EtOAc (425 nm) for dye **6d**. The maximum solvatochromism is found for dye **6d** 27 nm (computationally) while 15 nm (experimentally). Also the largest wavelength difference between the experimental absorption maxima and computed vertical excitation is 14 nm (DMF) for dye **6a**, 28 nm (acetone) for dye **6b**, 34 nm (THF) for dye **6c** and 106 nm (DMF) for dye **6d.**

Experimentally obtained fluorescence emission spectral data and emission computed from TD-B3LYP/6-31G (d)

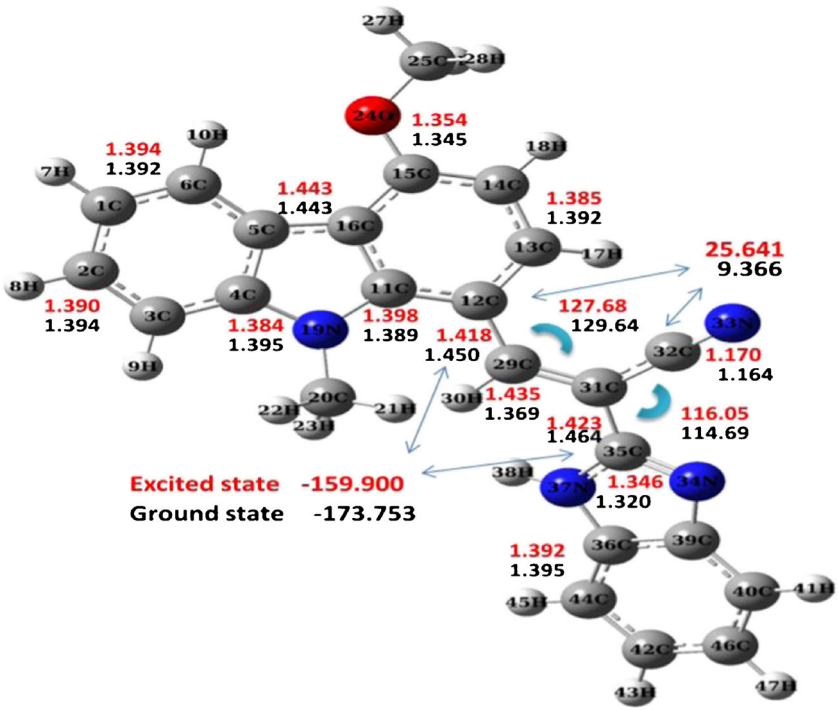

Fig. 11 Optimized geometry parameters of dye **6c** in Chloroform solvent in the ground and excited state (bond lengths are in Å, angles are in°)

Table 10 Mulliken charge distribution for dyes **6a, 6b, 6c** and **6d** in the ground state (GS) and excited state (ES) optimized geometry in chloroform

Atom no.	dye 6a		dye 6b		dye 6c		dye 6d	
	GS	ES	GS	ES	GS	ES	GS	ES
C_{11}	0.249	0.203	0.240	0.221	0.237	0.223	0.239	0.261
C_{12}	0.170	0.166	0.171	0.175	0.169	0.183	0.170	0.073
C_{15}	0.332	0.343	0.327	0.330	0.325	0.329	0.326	0.310
C_{16}	−0.002	0.030	−0.000	0.014	0.000	0.007	0.000	0.020
N_{19}	−0.639	−0.639	−0.639	−0.637	−0.639	−0.635	−0.630	−0.647
C_{20}	−0.356	−0.352	−0.354	−0.352	−0.350	−0.349	−0.350	−0.335
O_{24}	−0.508	−0.509	−0.512	−0.509	−0.514	−0.509	−0.512	−0.515
C_{25}	−0.234	−0.234	−0.231	−0.232	−0.230	−0.232	−0.231	−0.226
C_{29}	−0.174	−0.160	−0.239	−0.229	−0.233	−0.238	−0.224	−0.256
C_{31}	0.100	0.096	0.111	0.092	0.102	0.067	0.081	0.146
N_{33}	−0.520	−0.526	−0.536	−0.540	−0.533	−0.544	−0.539	−0.518
$N_{35/34/}$ O_{45}	−0.516	−0.514	−0.532	−0.541	−0.501	−0.604	−0.418	−0.414
$N_{37/}$ S_{46}/O_{46}	–	–	0.219	0.211	−0.760	−0.761	−0.417	−0.413

computations are shown in Tables 1, 2, 3, and 4. Both the computational and experimentally obtained emission spectral data were showing solvatochromism in dye **6a, 6b** and **6c,** but both the results not showing solvatochromism for dye **6d.** The experimental emission wavelengths are in well agreement with those computed with a deviation ranging between 1 and 12 % in the solvents studied. The difference between experimental and computational emission wavelength was observed maximum for dye **6d** in acetonitrile solvent (12.43 % deviation) while minimum for dye **6b** in EtOAc solvent (0.15 % deviation).

Frontier Molecular Orbital's

To understand energies of different HOMO and LUMO's of these four push-pull dyes and their comparative electronic transition and charge delocalization their respective frontier molecular orbital's were studied. Table S1 to S4 shows the energies of different molecular orbital's involved in the electronic transitions in different solvents. It was observed that the first allowed and the strongest electron transitions with largest oscillator strength usually correspond almost exclusively to the transfer of an electron from HOMO→LUMO.

From the pictorial diagram of the molecular orbital's as shown in Fig. 12, it was found that electron densities on the HOMO's of all four dyes were largely located on the donor carbazole moiety and electron densities on the LUMO's were found localized on one of the benzene ring of carbazole ring bearing methoxy substituent and on the withdrawing malononitrile (**6a**), 2-cyanomethyl-1,3-benzthiazole (**6b**), 2-(cyanomethyl)benzimidazole **(6c)** and para-nitro benzyl cyanide (**6d**) moieties respectively. For dye **6a** the HOMO-LUMO gap is highest (3.277 eV) for chloroform solvent while it is lowest (3.256 eV) for DMF solvent. Thus it is lowered by 0.021 eV as solvent polarity increases. Similarly for dye **6b** highest HOMO-LUMO gap is for chloroform (3.141 eV) and lowest is for DMF (3.124 eV) and it is lowered by 0.017 eV as solvent polarity increases. Similar trend is observed for dye **6c** and dye **6d**, for which HOMO-LUMO gap again decreases as solvent polarity increases. It is decreases by 0.017 and 0.048 eV for dye **6c** and dye **6d** respectively from non-polar to polar solvent.

Optimized Geometry of Dye 6d in Ground and Excited State

Dye **6d** was optimized in ground as well as excited state and it is observed that the withdrawing para-nitro benzyl cyanide moiety turns completely perpendicular to the donating carbazole ring in the excited state (Fig. 13). This change in the geometry also reflects into the charge delocalization. As described previously (table 6) this dye **6d** (1-styryl derivative) unexpectedly showing blue shifted emission than their 3-styryl partner. Also improper Mulliken charge delocalization for atom number O_{24}, N_{19}, N_{33}, O_{45} and O_{46} is observed. In the excited state, charge on atom number O_{24} and N_{19} should become more positive and charge on atom number N_{33}, O_{45} and O_{46} should become more negative, but this trend is observed reverse for this dye. Also there is increase in bond length of C_{31}-C_{32} and no change in bond length for C_{32}-C_{33} which is unexpected. But there is increase in bond length of O_{44}-O_{45} and O_{44}-O_{46} as expected, similarly decrease in bond length of C_{15}-O_{24} as expected which is not observed in the case of other three dyes, suggesting that in this dye **6d** the possible charge delocalization is originates from O_{24} and not from N_{19}.

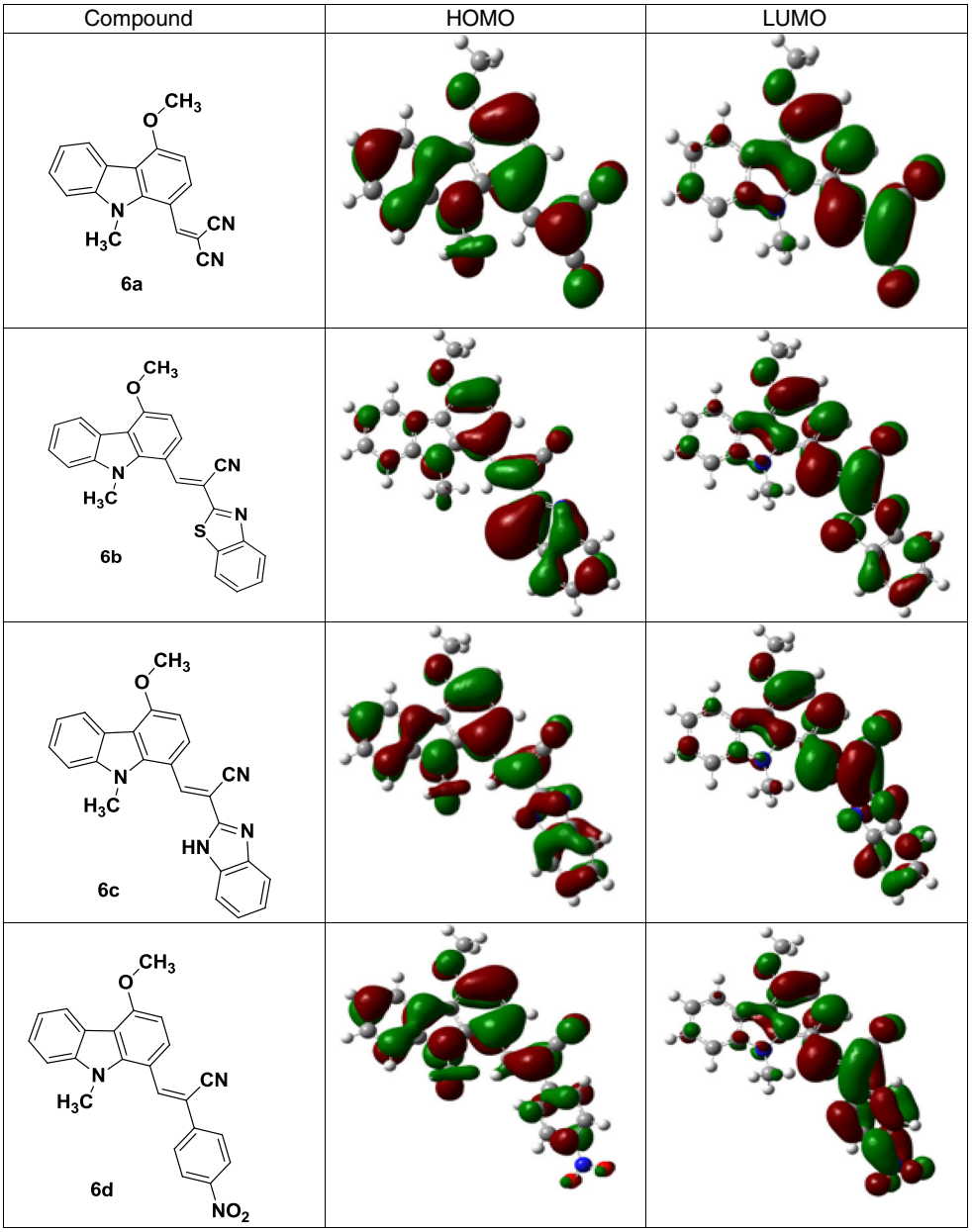

Fig. 12 Frontier molecular orbital's of dyes **6a**, **6b**, **6c** and **6c** in the ground state

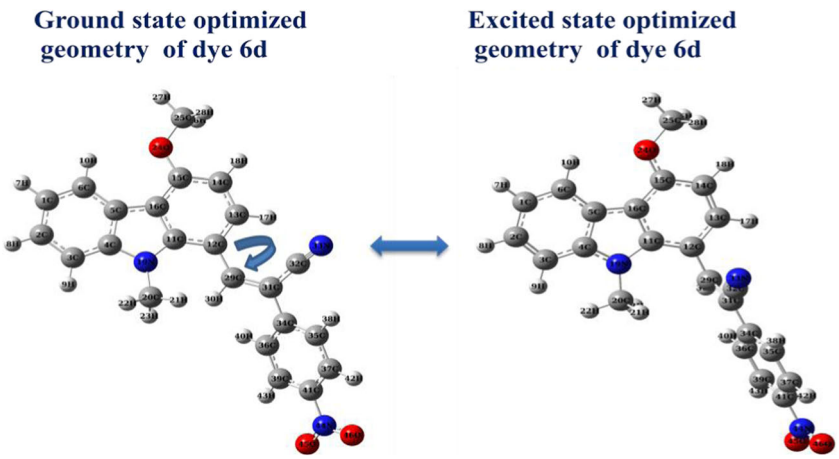

Fig. 13 Ground and excited state optimized geometry of dye **6d** in chloroform

Conclusion

In this chapter, we have successfully synthesized fluorescent styryl derivatives from compound **3** by an efficient and simple method. The dyes **6b** and **6c** shows good yellow solid state fluorescence, while in solution state dye **6a** has remarkable emission intensity. The solvatochromism and solvatofluorism study show that bathochromic shift in absorption is observed for chloroform and DCM, while bathochromic shift in emission is observed for DMF with strong emission intensity for dyes **6a–6c**, but in dye **6d** a remarkable shift in emission maxima is observed in EtOAc. Dye **6d** has highest Stokes shift in majority of solvent among the series. All the synthesized dyes have polar ground state than the excited state. The 1-styryl and 3-styryl derivatives (previously reported) were compared and it is found that the styryl derivatives at 1 position are red shifted than the styryl derivatives at 3 position.

The computed absorption and emission wavelengths are in good agreement with the experimental results. The electron densities on the HOMO's are of these dyes are largely located on the donating carbazole ring and that of LUMO's are found localized on withdrawing moieties. The abnormal behaviour of dye **6d** in its experimental photophysical properties is proved computationally where the withdrawing para-nitro benzyl cyanide ring is found completely perpendicular to the donating carbazole ring which disturbing the normal charge delocalization. In short the experimental observations are very well supported by the computation also and these push-pull dyes can be used promising candidate for various applications in electronic and photonic devices and organic light emitting diodes.

Acknowledgments The author is very much thankful to University Grant Commission (UGC), New Delhi, India for providing financial support and to IIT Mumbai for recording the ^{1}H NMR, ^{13}C NMR, and mass spectra.

References

1. Chilton JA, Goosey MT (1995) Special Polymers for Electronics and Optoelectronics. Champman and Hall, London
2. Law KY (1993) Chem Rev 93:449–486
3. Krotkus S, Kazlauskas K, Miasojedovas A, Gruodis A, Tomkeviciene A, Grazulevicius JV, Jursenas SJ (2012) Phys Chem C 116:7561–7572
4. Jiang W, Duan L, Qiao J, Dong G, Zhang D, Wang L, Qiu YJ (2011) Mater Chem 21:4918–4926
5. Hsieh BR, Litt MR (1985) Macromolecules 18:1388–1394
6. Park JH, Koh T, Do Y, Lee MH, Yoo SJ (2012) Poly Sci Part A 50: 2356–2365
7. Oshima R, Uryu T, Seno M (1985) Macromolecules 18:1043–1045
8. Uryu T, Ohkawa H, Oshima R (1987) Macromolecules 20:712–716
9. Shattuck MD (1969) Vahtra. U US Patent 3:484,327
10. Hu CJ, Oshima R, Sato S, Seno MJ (1988) Polym Sci C: Polym Lett 26:441–450
11. Ho MS, Barrett C, Paterson J, Esteghamatian M, Natansohn A, Rochon P (1996) Macromolecules 29:4613–4618
12. V. D. Gupta: A. B. Tathe; V. S. Padalkar; V. S. Patil; K. R. Phatangare; P. G. Umape; N. Sekar *Journal of fluorescence* **2013**, pp 1-18.
13. Shen J, Yang X, Huang T, Lin JT, Ke T, Chen W (2007) C.; Ming-Chang P. Yeh. Adv Funct Mater 17:983–995
14. Li, L.; Yuan, N.; Wang, P.; Wu, Y.; Song, Y.; Chen, Z.; He, C. *J. Phys. Org. Chem.* **2012**, 2937-2944.
15. Yang Z, Chi Z, Xu B, Li H, Zhang X, Li X, Liu S, Zhang Y, Xu JJ (2010) Mater Chem 20:7352–7359
16. Leclerc N, Michaud A, Sirois K, Morin JF, Leclerc M (2006) Adv Funct Mater 16:1694–1704
17. Blouin N, Michaud A, Leclerc M (2007) Adv Mater 19:2295–2300
18. Blouin N, Michaud A, Gendron D, Wakim S, Blair E, Neagu-Plesu R, Belletête M, Durocher G, Tao Y, Leclerc MJ (2008) Am Chem Soc 130:732–742
19. Zou Y, Gendron D, Badrou-Aïch R, Najari A, Tao Y, Leclerc M (2009) Macromolecules 42:2891–2894
20. Park SH, Roy A, Beaupré S, Cho S, Coates N, Moon JS, Moses D, Leclerc M, Lee K, Heeger AJ (2009) Nat Photonics 3:297–303
21. Lai H, Hong J, Liu P, Yuan C (2012) Li. Y.; Fang, Q. RSC Advances 2:2427–2432
22. Wakim S, Beaupré S, Blouin N, Aich B, Rodman S, Gaudiana R, Tao Y, Leclerc MJ (2009) Mater Chem 19:5351–5358
23. Chang CC, Kuo IC, Lin JJ, Lu YC, Chen CT, Back HT, Lou PJ, Chang TC (2004) Chem Biodivers 1:1377–1384
24. Fei X, Gu Y, Li C, Yang XJ (2012) Fluoresc 22:807–814
25. Lu M, Zhu Y, Ma K, Cao L, Wang K (2012) Spectrochim Acta A Mol Biomol Spectrosc 95:128–134
26. Zhang Q, Gao Y, Zhang S, Wu J, Zhou H, Yang J (2012) Taob.; Tia, Y. Dalton Trans 41:7067–7072
27. Eum SJ, Kwon HJ, Kim SM, Yoon SS (2011) WO 2001/105700 A1
28. Ramkumar S, Manoharan S, Anandan S (2012) Dyes Pigm 94:503–511
29. Li L, Wu Y, Zhou Q, Chunying He CJ (2012) Phys Org Chem 25: 362–372
30. Yang Z, Zhao N, Sun Y, Miao F, Liu Y, Liu X, Zhang Y, Ai W, Song S, Shen X, Yu X, Sun J, Wong W (2012) Chem Commun 48:3442–3444
31. Gupta VD, Padalkar VS, Phatangare KR, Patil VS, Umape PG, Sekar N (2011) Dyes Pigm 88:378–384
32. Gupta VD, Tathe AB, Padalkar VS, Patil VS, Phatangare KR, Umape PG, Ramasami P.Sekar NJ (2012) Fluoresc 22:807–814
33. Vidya S, Ravikumar C, Hubert JI, Kumaradhas P, Devipriyac B, Raju K. Vibrational spectra and structural studies of nonlinear optical crystal ammonium D, L-tartrate: a density functional theoretical Approach. J Raman Spectrosc 2011; 42:676e84.
34. Treutler O, Ahlrichs R. Efficient molecular numerical integration schemes. J Chem Phys 1995; 102:346e54.
35. Hehre WJ, Radom L (1986) Schleyer PvR, Pople J. Ab initio molecular orbital theory. Wiley, New York
36. Bauernschmitt R, Ahlrichs R. Treatment of electronic excitations within the adiabatic approximation of time dependent density functional theory. ChemPhys Lett 1996; 256: 454e64
37. Furche F, Rappaport D (2005) Density functional theory for excited states: equilibrium structure and electronic spectra. In: Olivucci M (ed) Compu-tational Photochemistry, vol 16. Elsevier, Amsterdam [Chapter 3]
38. Valeur B (2001) Molecular fluorescence: principles and applications. Weinheim, Wiley-VCH Verlag

39. Cossi M, Barone V, Cammi R, Tomasi J. Ab initio study of solvated mole-cules: a new implementation of the polarizable continuum model. Chem Phys Lett 1996; 255: 327e35
40. Tomasi J, Mennucci B, Cammi R. Quantum mechanical continuum salvation models. Chem Rev 2005; 105:2999e3094.
41. Umape P; Gawale Y; Sekar N. *J. Fluoresc. (in press)* DOI 10.1007/s10895-014-1389-9
42. Bakhshiev NG (1964) Opt Spektrosk 16:821–832
43. Kawski A (1966) Acta Phys Pol 29:507–518
44. Chamma A, Viallet PCR (1970) Acad Sci Ser C 270:1901–1904
45. Kawski A (1964) Naturwissenschaften 51:82–83